A drought index accounting for snow

Staudinger, Maria ; Stahl, Kerstin ; Seibert, Jan

Abstract: The Standardized Precipitation Index (SPI) is the most widely used index to characterize droughts that are related to precipitation deficiencies. However, the SPI does not always deliver the relevant information for hydrological drought management particularly in snow-influenced catchments. If precipitation is temporarily stored as snow, then there is a significant difference between meteorological and hydrological drought because the delayed release of melt water to the stream. We introduce an extension to the SPI, the Standardized Snow Melt and Rain Index (SMRI), that accounts for rain and snow melt deficits, which effectively influence streamflow. The SMRI can be derived without snow data, using temperature and precipitation to model snow. The value of the new index is illustrated for seven Swiss catchments with different degrees of snow influence. In particular for catchments with a larger component of snowmelt in runoff generation, the SMRI was found to be a worthwhile complementary index to the SPI to characterize streamflow droughts.

A drought index accounting for snow

Maria Staudinger[1], Kerstin Stahl[2], and Jan Seibert[1,3]

[1]Department of Geography, University of Zurich, Zurich, Switzerland, [2]Faculty of Environment and Natural Resources, University of Freiburg, Freiburg, Germany, [3]Department of Earth Sciences, Uppsala University, Sweden

Abstract The Standardized Precipitation Index (*SPI*) is the most widely used index to characterize droughts that are related to precipitation deficiencies. However, the *SPI* does not always deliver the relevant information for hydrological drought management particularly in snow-influenced catchments. If precipitation is temporarily stored as snow, then there is a significant difference between meteorological and hydrological drought because the delayed release of melt water to the stream. We introduce an extension to the *SPI*, the Standardized Snow Melt and Rain Index (*SMRI*), that accounts for rain and snow melt deficits, which effectively influence streamflow. The *SMRI* can be derived without snow data, using temperature and precipitation to model snow. The value of the new index is illustrated for seven Swiss catchments with different degrees of snow influence. In particular for catchments with a larger component of snowmelt in runoff generation, the *SMRI* was found to be a worthwhile complementary index to the *SPI* to characterize streamflow droughts.

1. Introduction

Droughts always originate from a lack of precipitation. In some regions, high temperatures and evapotranspiration are additional important drivers of soil moisture and hydrological droughts. In contrast to these drought processes that occur in summer, the storage of precipitation as ice and snow can act as a key moderator of hydrological drought. In particular, streamflow droughts are often related to the presence or absence of snow in the preceding winter period and winter droughts can occur despite large amounts of precipitation, if the precipitation falls as snow. *Van Loon and Van Lanen* [2012] distinguish between six different hydrological drought types according to their development (classical rainfall deficit drought, rain-to-snow-season drought, wet-to-dry-season drought, cold snow season drought, warm snow season drought, and composite drought). Since hydrological droughts can have severe impacts on river ecology, water supply, energy production, or navigation, there is a need to monitor these droughts.

Drought monitoring requires indicators that are general enough to be widely applicable, but specific enough to capture the type of drought relevant to the region and variable of interest. The development of such indicators in the United States is summarized by *Heim* [2002]. There are only a few indices that consider snow explicitly, one of these for example, is the surface water supply index (*SWSI*) [*Shafer and Dezman*, 1982; *Doesken et al.*, 1991]. The Standardized Precipitation Index (*SPI*) is an indicator for drought that was first introduced by *McKee et al.* [1993]. Since its introduction, the *SPI* has been applied in many studies, in operational drought monitoring in the present, and also in scenario predictions of drought for climate change impact assessment [e.g., *Ji and Peters*, 2003; *Ghosh and Mujumdar*, 2007; *Naresh Kumar et al.*, 2009; *Orlowsky and Seneviratne*, 2012]. A major advantage of the *SPI* compared to other drought indices is that it requires only precipitation data to describe drought severity. It is calculated based on a theoretical probability distribution fitted to the long-term precipitation record aggregated over a chosen preceding period. This probability distribution is then transformed into a normal distribution so that the mean *SPI* is zero. Positive *SPI* values indicate greater than mean precipitation, and negative values indicate less than mean precipitation. As the *SPI* is standardized, wetter and drier climates are represented in the same way allowing for regional comparison studies [*Hayes et al.*, 1999].

Different precipitation aggregation periods can reflect the impact of drought as it propagates through the hydrological cycle into soil, streamflow, and groundwater. Soil moisture conditions are related to precipitation anomalies on a relatively short scale, whereas streamflow for instance, reflects longer-term precipitation anomalies [*Hayes et al.*, 1999]. With the right aggregation time, a climatic drought index such as the *SPI* may also be a suitable indicator for hydrological droughts. The US Drought Monitor, for example, uses composite

Table 1. Catchment Properties [*FOEN*, 2012]

Catchment Number	Name	Area (km^2)	Mean Elevation (m a.s.l.)[a]	Elevation Range (m a.s.l.)	Regime	Snow/Precipitation[b] (%)
1	Mentue	105.0	679	445–927	Pluvial	4.8
2	Sense	352.0	1068	548–2189	Pluvio-nival	11.7
3	Sitter	74.2	1252	769–2501	Nival	22.7
4	Allenbach	28.8	1856	1297–2762	Nival	33.7
5	Riale di Calneggia	24.0	1996	885–2921	Nival	34.3
6	Ova da Cluozza	26.9	2368	1508–3165	Nival	42.2
7	Dischma	43.3	2372	1668–3146	Nival	44.7

[a]a.s.l., above sea level.
[b]Percent of snow in precipitation is calculated as the ratio of precipitation on days with air temperatures below 0°C and precipitation from the entire observational period.

drought indices with a focus on short *SPI* aggregation periods for warnings about agricultural drought impacts and composite indices with a focus on longer *SPI* aggregation periods for warnings about hydrological drought impacts (droughtmonitor.unl.edu). Several studies have investigated the time lag between SPI and streamflow drought in order to find the most suitable *SPI* aggregation period linked to hydrological drought characterization. Some researchers have determined such a time lag between meteorological drought and streamflow drought [*Haslinger et al.*, 2014], while others found strong dependencies apart of areas that have a large groundwater storage [*Haslinger et al.*, 2014] or at times of snow storage [*Shukla and Wood*, 2008; *Vidal et al.*, 2010].

To create a methodologically consistent indicator of hydrological droughts, several studies have transferred the *SPI* approach to observed and modeled hydrological variables. *López-Moreno et al.* [2009] and *Vicente-Serrano et al.* [2011] applied the SPI concept to observed streamflow in Spain, introducing a standardized streamflow index (*SSI*). *Shukla and Wood* [2008] derived a standardized runoff index (*SRI*) for monthly aggregations of modeled daily grid cell runoff, which consisted of modeled surface runoff and base flow (subsurface flow). The results were *SRI* maps for the entire United States based on the grid cells of a large-scale hydrological model. *Vidal et al.* [2010] applied the approach to hydrological model output for France, but instead of grid cell runoff they calculated a standardized flow index for the routed streamflow. *Shukla and Wood* [2008] and *Vidal et al.* [2010] compared their derived hydrological indices with the traditional *SPI* in order to explore the time lag of the drought propagation through the hydrological cycle. They concluded that a standardized runoff index can complement the *SPI* especially in periods when variables other than precipitation become more important, e.g., periods of snow accumulation and melt. While the advantage is that modeled runoff considers precipitation, temperature, and radiation as well as information about the variability of vegetation, soil, and terrain characteristics, it cannot be validated. Only runoff routed to the outlet of a catchment, i.e. the streamflow, can be gauged and thus validated. Unfortunately, in many catchments, streamflow data are influenced by human impacts or are not available for periods long enough to calculate an *SSI* based on observations.

The *SPI* can be modified to indicate a hydrological drought rather than a precipitation drought without the full complexity of a hydrological model, by only accounting for first-order controls on catchment hydrology that affect drought. Recently, *Vicente-Serrano et al.* [2010] introduced an index that accounts for evapotranspiration as an important amplifier of drought and found this index to be useful for catchments in Spain. This study specifically aimed for a climatic drought index with low data requirements which can serve as an indicator for hydrological drought in regions with a variable influence of snow. In such regions, e.g., mountain headwaters, streamflow is a major source of water use for water supply, energy production, and the ecology of mountain streams is vulnerable to drought. Therefore, this study uses a drought index based on observed streamflow, the *SSI*, as a benchmark against which to compare the climatic drought index *SPI* and the new Standardized Snow Melt and Rain Index (*SMRI*). The comparison is done for seven Swiss catchments with different amounts of snow melt contributions to streamflow.

2. Data and Methods

2.1. Data

Data from seven unregulated mesoscale catchments in Switzerland were used in this study (Table 1). The mean elevation for the different catchments ranges between 700 and 2400 m above sea level (a.s.l.). The catchment areas range between 20 and 350 km^2, and the estimated fraction of annual snow in precipitation

Table 2. Mean Values of F_{bench} for Different Aggregation Periods and All Catchments

Aggregation Time (months)	Mentue	Sense	Sitter	Riale di Calneggia	Allenbach	Ova da Cluozza	Dischma
Full period							
1	0.008	0.079	0.197	0.341	0.332	0.573	0.465
2	0.010	0.093	0.226	0.366	0.405	0.610	0.479
3	0.011	0.100	0.268	0.396	0.448	0.629	0.488
4	0.012	0.104	0.284	0.424	0.468	0.639	0.492
6	0.012	0.107	0.261	0.438	0.476	0.620	0.475
12	−0.003	0.029	0.073	0.181	0.182	0.333	0.187
Dry periods							
1	0.004	0.059	0.216	0.386	0.296	0.635	0.514
2	0.004	0.065	0.215	0.390	0.361	0.667	0.541
3	0.005	0.064	0.245	0.412	0.393	0.679	0.558
4	0.008	0.067	0.251	0.436	0.412	0.685	0.553
6	0.011	0.083	0.265	0.438	0.453	0.649	0.498
12	−0.009	0.026	0.097	0.192	0.164	0.352	0.193

ranges between 5 and 45% (Table 1). Daily precipitation and temperature data were derived from the grid products RhiresD and TabsD [*Frei*, 2013] provided by MeteoSwiss (2013). Both grid products are based on the interpolation of the daily anomalies of a dense network of meteorological records on a spatial background climatology. The daily grids have a spatial resolution of 2 km × 2 km and cover the period 1971–2011. For this study, catchment averages of precipitation and temperature were computed. Observed time series of daily mean streamflow were available for the same period (1971–2011) for all catchments. [*Federal Office for the Environment (FOEN)*, 2012].

2.2. Probability Distribution Selection for SPI and SSI

For the calculation of standardized drought indices, a theoretical distribution has to be chosen. The *SPI* has often been calculated based on the Gamma distribution, even though some authors claim that other distributions like the Pearson type III distribution might be more suitable [e.g., *Guttman*, 1999]. We tested different theoretical distributions as suggested by *Vicente-Serrano et al.* [2010, 2011]. The best fit for all variables on average was found for the Pearson type III distribution, which then served as a basis for all index calculations (*SPI*, *SSI*, and the new *SMRI*). The parameters of the distribution were estimated using the L-moments method as described by *Hosking* [1990].

2.3. The Standardized Melt and Rainfall Index (*SMRI*)

The new *SMRI* was calculated similarly to SPI and SSI, but from the daily sum of snow melt and rain (*MR*). To obtain daily snow melt amounts, a commonly used snow model that only requires temperature data in addition to precipitation was first applied. While any snow model or derivation of snow melt could be used to calculate the index, the model used here consists of a snow accumulation component based on a threshold temperature and of a snow melt component based on a degree-day approach allowing for storage of up to 10% of the current simulated snow water equivalent and refreezing of liquid water in the snow pack (at a reduced rate compared to melting) [e.g., *Bergström et al.*, 1992] (a detailed description can be found in Appendix A). The variable *MR* was then transformed into the index *SMRI* using the Pearson type III distribution.

In order to explore the level of local parameterization needed, three parameter set ensembles were tested: the first parameter set ensemble (Set 1) assumed no prior knowledge (10,000 random parameter sets), the second set (Set 2) assumed some regional knowledge, and the third set (Set 3) assumed specific catchment knowledge. Set 1 was derived from a Monte Carlo analysis, where 10,000 parameter combinations were tested for the snow model. The sample for the Monte Carlo simulations was created using Sobol' sequences (R Package randtoolbox, CRAN, 2012). For the parameter sets, we chose typical parameter ranges [*Seibert*, 1999] for the threshold temperature between −2.5 and 2.5°C, for the degree-day factor between 1 and 6 mm°C^{-1}day^{-1} [*Esko*, 1980; *Seibert*, 1999; *Hock*, 2003; *Merz and Blöschl*, 2004], for the refreezing coefficient between 0 and 0.1.

Set 2 and 3 came from calibrating a full hydrological model, which contains apart of the same snow model routine also soil and groundwater response and routing routines (HBV model in the version HBVlight

[*Seibert and Vis*, 2012]). The model was automatically calibrated to observed streamflow for each catchment over the period 1971–2011. For the calibration, a genetic optimization algorithm with subsequent steepest gradient tuning [*Seibert*, 2000] was used. Calibration trials (100) were performed, which resulted in 100 optimized parameter sets for each catchment according to a combination of Nash-Sutcliffe model efficiency and volume error [*Lindström et al.*, 1997], where the weighting factor for the volume error was set to 0.1, as recommended by *Lindström et al.* [1997] and *Lindström* [1997]. The same parameter ranges that were used in the Monte Carlo simulations for Set 1 were used for the calibration. Set 2 was the resulting 100 optimized parameter sets for each catchment. Finally, for each catchment a so called regional parameter set (Set 3) was composed, consisting of Set 2 of all other catchments (i.e., here $100 \times 6 = 600$).

These snow model parameter values were then used to compute *SM* and subsequently *SMRI*.

2.4. Application and Comparison of *SMRI* to *SPI* and *SSI*

All indices were calculated for different aggregation periods (1, 2, 3, 4, 6, and 12 months), referred to as, for instance *SMRI*−6 for the *SMRI* calculated based on a 6 months preceding aggregation period. If no aggregation period is specified, results refer to all aggregation periods.

To compare the new *SMRI* as well as the *SPI* to our variable of interest, the *SSI*, a benchmark model efficiency F_{bench} (equation (1)) [*Schaefli and Gupta*, 2007] was used as one measure of comparison. F_{bench} was calculated as the ratio of the quadratic absolute errors; subtracting the ratio from one transforms it to a range of minus infinity to one. A value of one for F_{bench} corresponds to a perfect fit of the *SSI* and *SMRI*. Values larger than zero indicate that the *SMRI* is closer to the *SSI* than the *SPI* and values below zero indicate that the *SPI* is closer to the *SSI* than the *SMRI*.

$$F_{bench} = 1 - \frac{\sum \left(x_{SSI}(t) - x_{SMRI}(t)\right)^2}{\sum \left(x_{SSI}(t) - x_{SPI}(t)\right)^2} \tag{1}$$

F_{bench} was calculated for both the entire index time series (1971–2011) as well as for the hydrological dry periods only ($SSI < 0$).

In addition to this general evaluation, we looked at two historical drought events in particular: the summer drought of 2003 [*Rebetez et al.*, 2006] as well as the spring drought of 2011. The summer drought 2003 was caused by a lack of precipitation and, due to extremely high temperatures, also high evapotranspiration rates. The drought in spring 2011 resulted from a preceding winter with little precipitation and thus little snow accumulation in combination with relatively high temperatures during spring time.

2.5. Sensitivity to Elevation Distribution

The *SMRI* series were first computed for the mean catchment elevations. To assess how representative this lumped approach is, the *SMRI* computation was repeated in a semidistributed way: each catchment was divided into elevation zones of 100 m. For each elevation zone, both the fraction of the elevation zone of the catchment as well as the temperature change according to a fixed lapse rate of $0.6°$C/100m were calculated. From the area-weighted mean of *SM*, the $SMRI_{elev}$ was derived. Finally, the $SMRI_{elev}$ was compared to the *SMRI* for aggregation periods of 1 and 3 months using F_{bench} (equation (1)). While the consideration of elevation zones changes the temporal distribution of snow accumulation and melt, for aggregation periods that are longer than the annual snow period this has no significant impact.

3. Results

The values for F_{bench}, derived from Set 1, were in most catchments and for most parameter sets greater than zero, which means that the *SMRI* was closer to the *SSI* than the *SPI* for both the entire period and the dry periods (Figure 1, Table 2). For the catchment with the smallest snow/precipitation ratio, the *SPI* and the *SMRI* were comparable. However, the difference increased systematically with increasing snow influence on the streamflow regime for both the entire period as well as for the dry periods only (Figure 1). The values for F_{bench} were on average slightly lower for the simulations which were based on parameters with prior knowledge (Sets 2 and 3) and the spread was smaller (Figure 2).
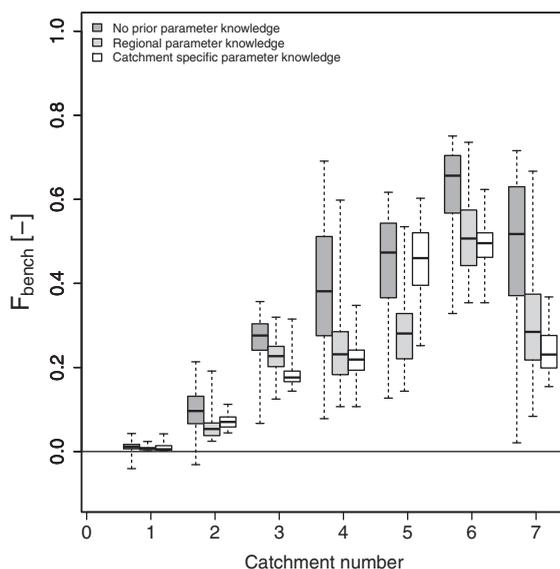
There were also seasonal patterns in F_{bench} (Figure 3): for the two catchments with the highest average snow contribution ($>30\%$), F_{bench} decreases slightly in the summer months. For the catchments with
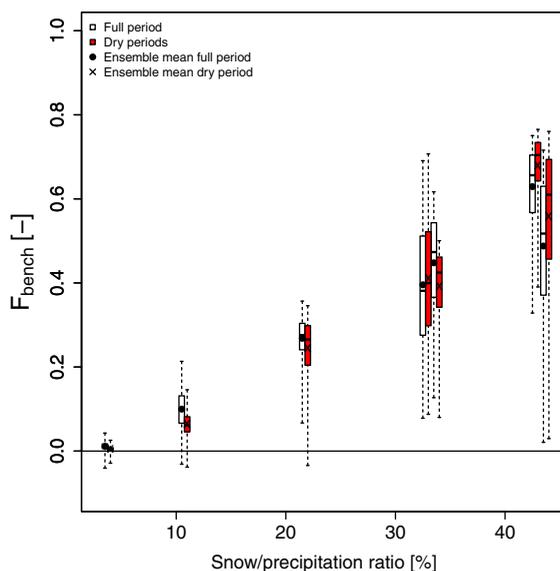
Figure 1. Distributions of the measure of comparison F_{bench} for snow model parameter Set 1 for drought indices with an aggregation period of 3 months. Each pair of boxes (white plus red) represents one catchment. Additionally, the measure of comparison of the ensemble mean is shown. The whiskers of a boxplot extend to the minimum and the maximum values, the box extends from the 25th to the 75th percentile and the bar shows the median.
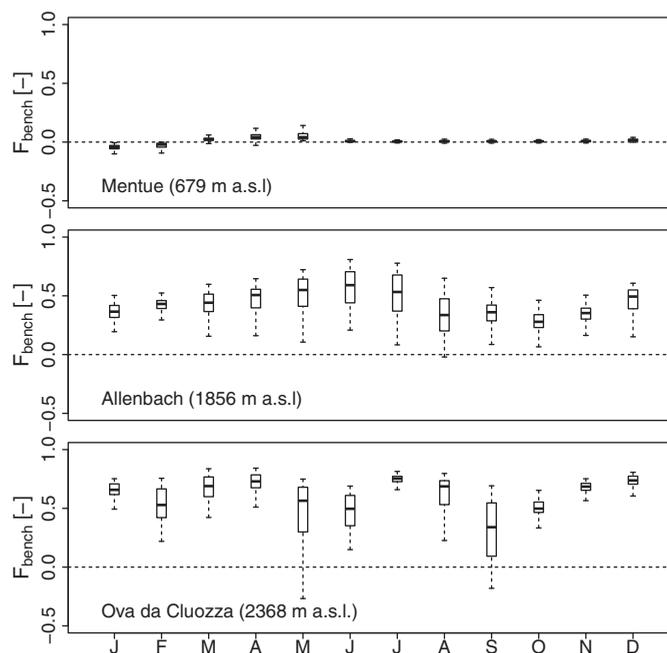
between 10 and 23% average snow ratio, during the melt period (April, May, and June), the hydrological droughts were closer represented by the *SMRI* than by the *SPI*. The Mentue catchment with a pluvial streamflow regime shows a closer representation of the *SSI* by the *SPI* in January and February while for the rest of the year by the *SMRI*.

Figures 4 and 5 show the droughts of 2003 and 2011 for the Ova da Cluozza catchment (nival). In 2003, the *SMRI* was closer to the *SSI* than the *SPI* regardless of the aggregation period. However, the ensemble mean overestimated the streamflow drought for the aggregation periods of 1–4 months. *SMRI*−6 and *SSI*−6 were similar regarding both severity and duration. The duration of the drought was captured well for all aggregation periods. While the *SPI* indicated severe droughts with values below −1.5, both *SSI* and *SMRI* indicated a less severe drought. For 2011, the ensemble mean

of the *SMRI* mimicked the *SSI* in all aggregation periods. Here again, the *SPI* indicates more severe droughts than the *SSI* and *SMRI*.

Figures 6 and 7 show onset and end of the droughts in all catchments. While in the Mentue and Sense catchments, *SPI*−3 and *SMRI*−3 fail to identify the start and end of the hydrological summer drought of 2003 as indicated by the *SSI*−3, for the nival Sitter, Allenbach, and Riale di Calneggia catchments they better describe the start and end of the drought. For the two catchments with the highest elevation (Ova da Cluozza and Dischma), the *SMRI* matches the end of the drought as indicated by the *SSI*−3, but defines its start later. However, the *SMRI*−3 indicates the start of the drought about 1 month earlier, i.e. closer to the *SSI* than the *SPI*−3.

For the Mentue and Sense catchments, which generally have little snow, neither the *SPI* nor the *SMRI* capture the timing of the hydrological spring drought in 2011; also for the Sitter and Allenbach catchments, *SPI* and *SMRI* are similar. For catchments with the most snow, the *SMRI* closer matches *SSI* than the *SPI* regarding the start and the end of the spring drought. Different thresholds that define different severities of droughts could be applied, which also bring the *SMRI* closer to the *SSI* than the *SPI*.

Including different elevation zones of a catchment improved *SMRI*−1 and *SMRI*−3 (Figure 8). The strongest improvement was found for catchments with mean catchment elevations from 1000 to 2000 m a.s.l. (Sense, Sitter, Allenach, Riale di Calneggia). However, the relative ranking of the

Figure 2. Distributions of the measure of comparison F_{bench} for the three different snow model parameter sets for drought indices with an aggregation period of 3 months. Boxplots as in Figure 1.

Figure 3. Distributions of the measure of comparison F_{bench} for each month, modeled with Set 1 for a catchment with little snow influence (top), a catchment with medium snow influence (middle), and a catchment with high snow influence (bottom). Boxplots as in Figure 1.

catchments' F_{bench} is similar for $SMRI$ and $SMRI_{elev}$. For the $SMRI-1$, the improvement when using elevation zones was slightly higher than for the $SMRI-3$. For both $SMRI-1$ and $SMRI-3$, a clear reduction of the spread in values was found when different elevation zones were considered.

4. Discussion

4.1. Uncertainties From Model and Index Standardization

The proposed $SMRI$ is an index that is calculated in a two-step process; i.e. first a model is applied that accounts for the dominant process that affects severity and timing of hydrological drought, and then the output of this model is transformed into the index. In the mountainous regions of interest in this study, the process first modeled is the delayed storage and release of snow. As for similar approaches such as the SRI, which used a hydrological model in the first step [*Shukla and Wood*, 2008] or the Standardized Precipitation and Evapotranspiration Index ($SPEI$), which uses an evapotranspiration estimation in the first step [*Vicente-Serrano et al.*, 2010, 2012], this two-step process means that the resulting index has multiple sources of uncertainty. The most important sources of uncertainty from the snow model are the parameterization of the degree-day model, the spatial discretization of elevation as well as data uncertainty. Model parameterization and spatial discretization were addressed by ensemble approaches using parameterizations stemming from no prior knowledge, regional knowledge, and specific catchment knowledge. The calculation of the actual index is then influenced by semiobjective decisions including that for a theoretical distribution function and finally the choice for an aggregation period to be used.

The Monte Carlo approach that was used is a common way to test the sensitivity to model parameterization [e.g., *Demaria et al.*, 2007]. The results showed variation in the performance of the $SMRI$. However, for the snow influenced catchments and for most parameter combinations, the entire parameter range resulted in an $SMRI$ that was much closer to a hydrological drought description than the SPI for both the entire observation period as well as for the dry periods only. For the catchments with less snow influence, there is no disadvantage compared to the SPI. Increasing the knowledge about the snow model parameters of a catchment decreased the uncertainty. However, there was not an increase but a slight decrease of the performance found. This decrease is counter-intuitive but might be explained by the fact that the prior knowledge parameters were derived by calibration of a full hydrological model. The optimal snow parameter values derived in this way might be model specific and not be those providing best results for the SMRI, when soil or groundwater were not considered. These results indicate that the use of an ensemble of random parameters actually might be the most appropriate approach after all. Overall, the parameterization of the snow model has only a minor influence on the systematic performance of the $SMRI$. Propagating an ensemble is generally a useful way to illustrate the degree of uncertainty that is associated with a model simulation [*Pappenberger and Beven*, 2004; *Montanari*, 2005; *Choi and Beven*, 2007]. An ensemble creates more robust results that depend less on a choice of the parameter values.
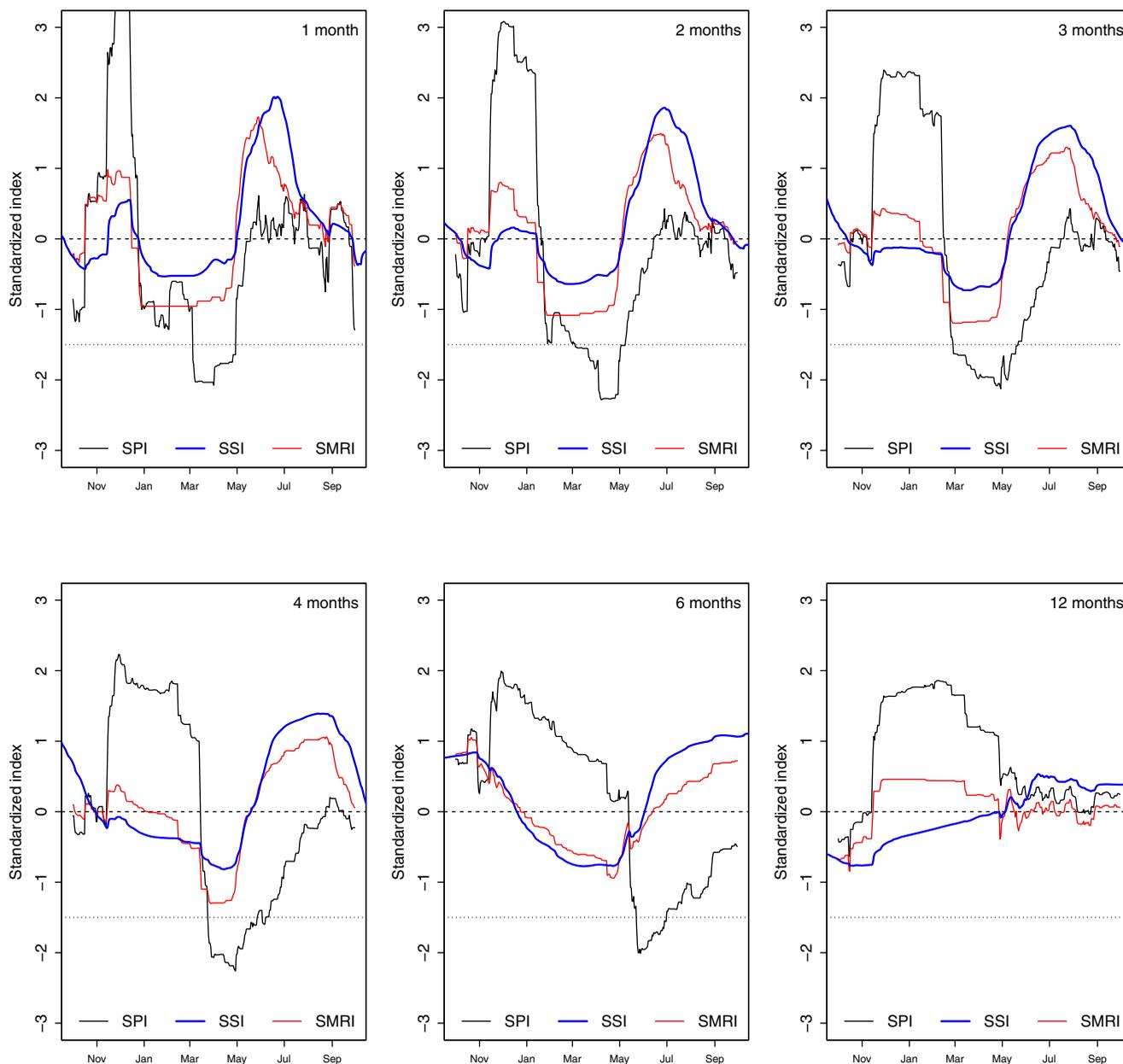
Using elevation zones in the melt model instead of a lumped mean elevation, improved the performance of the $SMRI$. The resulting reduction of the range of $SMRI$ values can be attributed to the explicit consideration of higher elevations. Here, the influence of the threshold temperature (see Appendix A) is smaller, thus

Figure 4. Standardized precipitation (*SPI*) (black), streamflow (*SSI*) (blue), and ensemble mean of the snow melt rain index (*SMRI*) (red) in daily resolution for six different accumulation periods during the summer drought 2003 for the nival Ova da Cluozza catchment.

causing a more stable snow cover and hence less variability in modeled snow melt. Still, when no information on the elevation distribution is available, the simpler approach of using the catchment mean elevation resulted in values of F_{bench} greater than zero, meaning the *SMRI* is closer to the *SSI* than the *SPI*. Other studies have found the use of only one lumped elevation zone to result in poor runoff simulations [*Uhlenbrook et al.*, 1999], the aggregation over at least a month in this study compensates the errors as the main effect if different elevation zones is a shift in the timing of snow melt.

Finally, the choice of the climate data input will affect the results. The snow model was driven with uncorrected precipitation data as corrected precipitation data are not a standard data product in Switzerland. Thus there can be errors due to precipitation undercatch—especially in winter when precipitation falls as snow [*Rasmussen et al.*, 2012]. However, the resulting bias affects the calculation of both indices, the *SMRI* and the *SPI*. Hence, the comparison of the indices and the results presented in this study should not be affected. The grid product used is the result of a well-validated interpolation from a dense network of
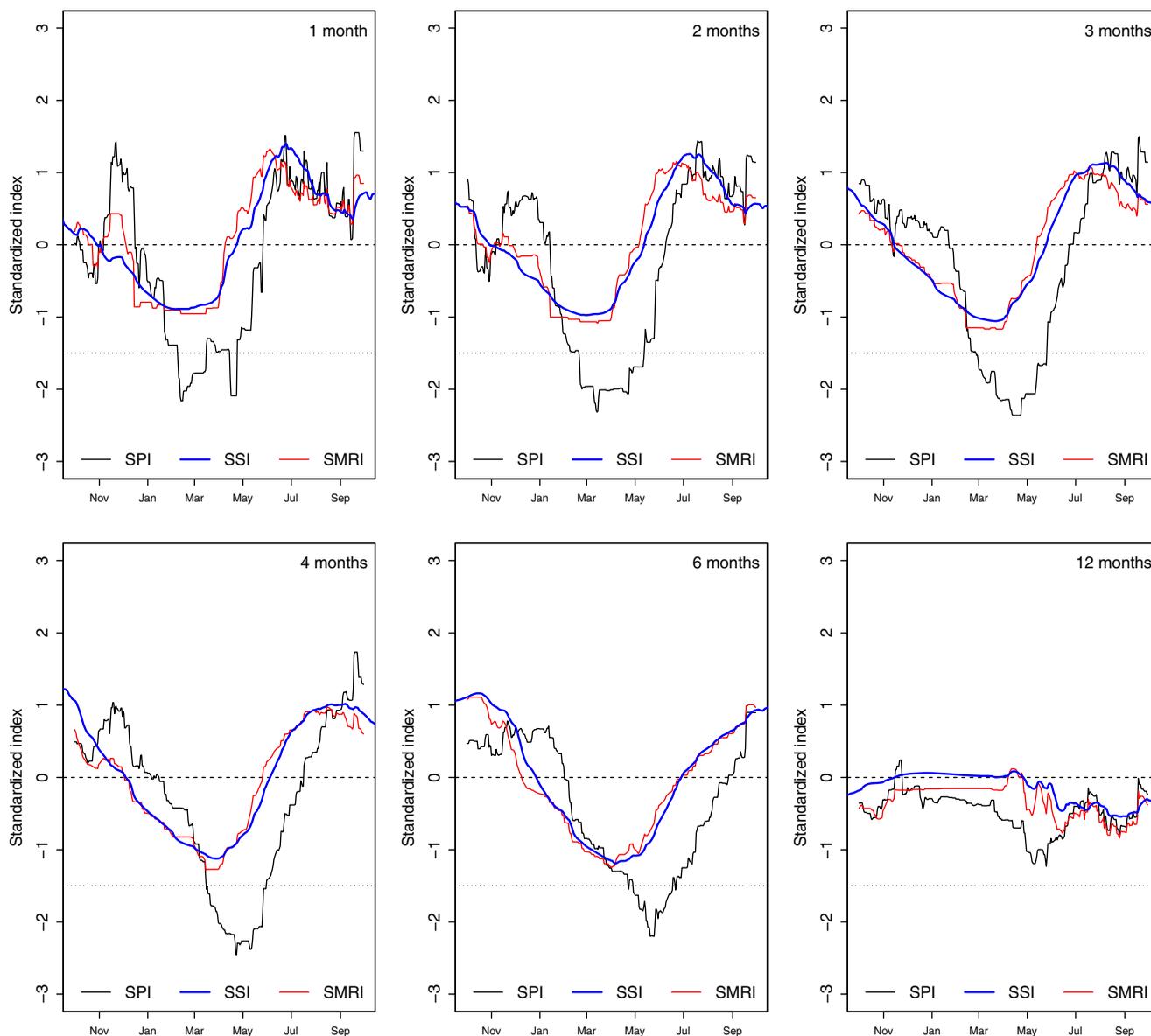
Figure 5. Standardized precipitation (*SPI*) (black), streamflow (*SSI*) (blue), and ensemble mean of the snow melt rain index (*SMRI*) (red) in daily resolution for six different accumulation periods during the spring drought 2011 for the nival Ova da Cluozza catchment.

climate stations. In other mountain regions of the world with less dense networks, interpolation will be more challenging and the errors may be higher.

The choice to include just one key process, i.e., snow accumulation and melt, in the model used to compute the *SMRI* has implications for the seasonal performance of the new index. The measure of comparison decreases in the months of May–August for the strongly snow influenced catchments. These are the months with the highest evapotranspiration, a process that was not modeled here, but could be considered in a similar way to the *SPEI* approach [*Vicente-Serrano et al.*, 2010] or in a full hydrological model using the *SRI* approach [*Shukla and Wood*, 2008]. For many snow-dominated catchments, including those used in this study, the performance gain by including processes other than snow is expected to be small. Despite the exclusion of evapotranspiration, over the entire year the *SMRI* was closer to the *SSI* than the *SPI* and particularly so in the months of snow melt. For the catchments with a pluvial regime, the difference between *SPI* and *SMRI* as an indicator for streamflow drought conditions is small or not existent.
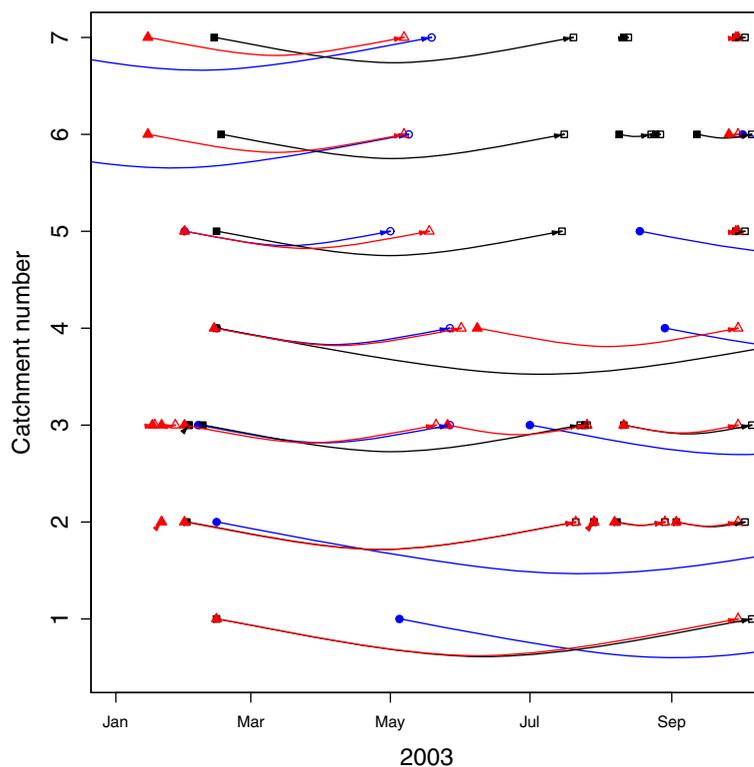
Figure 6. Starting dates of the summer drought 2003 (index <0) for standardized precipitation (*SPI*) (black), streamflow (*SSI*) (blue), and ensemble mean of the snow melt rain index (*SMRI*) (red) for the accumulation period of 3 months.

There has been some debate over the general concept of standardization which includes fitting a distribution to heavily skewed hydrometeorological data rather than using empirical percentiles. Empirical percentiles have been used mostly in studies that extract further drought characteristics below a threshold to define severity-area-duration or frequencies (and return periods) [e.g., *Cancelliere and Salas*, 2010; *van Vliet et al.*, 2012]. The concept of standardization has been used mostly for the analysis of entire time series and the propagation of drought through the hydrological cycle [e.g., *Hayes et al.*, 1999; *Shukla and Wood*, 2008]. In this study, we chose the *SPI* approach for consistency and compara-bility to currently used drought monitoring and early warning efforts. Even though *Vicente-Serrano et al.* [2011] found differences in mean, standard deviation, and in the estimation of extreme quantiles for the different distributions, the major dry and moist episodes, regardless of which distribution function was used, were clearly identified.

4.2. Application Potential

Similar to other existing drought indices, the new index can be calculated for different aggregation periods. The coevolution of *SPI*, *SSI*, and the new *SMRI* during two recent drought events showed that with an increasing aggregation period, the *SMRI* and *SPI* approximate each other for the studied catchments. The *SMRI* is thus considered useful to indicate streamflow droughts that occur in humid to semiarid mountain regions on a time scale below 1 year due to the seasonal character of snow storage. The *SMRI* seems especially suited for warm snow season droughts [*Van Loon and Van Lanen*, 2012] as the one in spring 2011.

The slightly greater performance difference between *SMRI*$_{elev}$-1 and *SMRI*-1 compared to *SMRI*$_{elev}$-3 and *SMRI*-3, especially in the catchments with an elevation range between 1000 and 2000 m a.s.l., can be explained with different phases of melt and accumulation that occur in the different elevation zones of a catchment. These differences matter less on longer aggregation time scales as net snow melt amounts for different elevation zones converge.

In the temperate humid climate of Switzerland, snow melt and precipitation occur in the same season, as rainfall is uniformly distributed over the year. This requires shorter aggregation periods to be considered for the calculation of the indices than in a Mediterranean climate, where wet and dry seasons are clearly separated. Where such a clear separation does not exist, other indices that include end-of season snow pack directly as, for example, the *SWSI*, will be less useful for drought assessment.

Ideally, an index also needs to be suitable for regional comparisons, i.e., easily applicable with distributed or gridded climate datasets and without further information needs. The *SWSI*, for instance, requires information on the different contributions of precipitation, snow, runoff, and reservoir storage as well as their
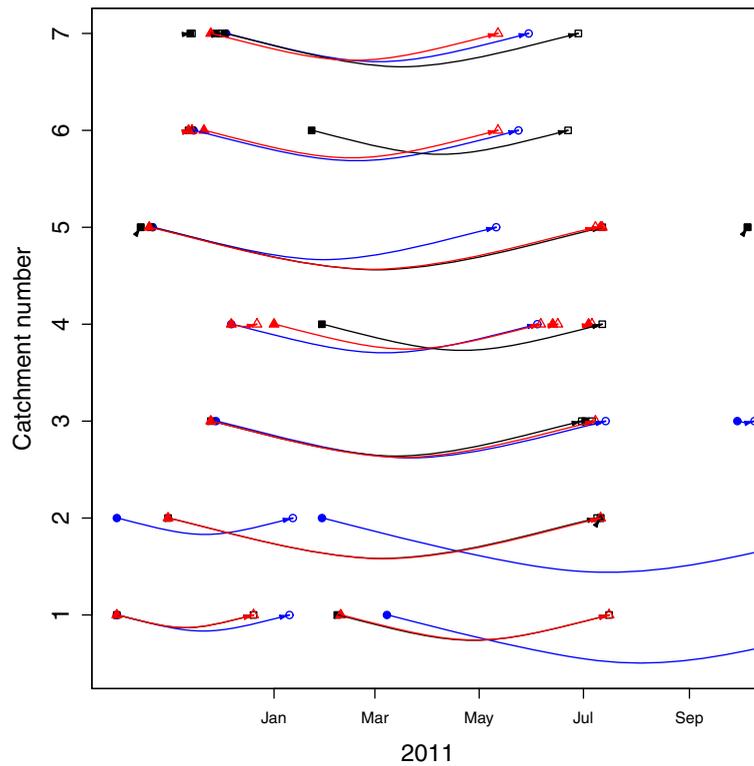
Figure 7. Starting dates of the spring drought 2011 (index <0) for standardized precipitation (*SPI*) (black), streamflow (*SSI*) (blue), and ensemble mean of the snow melt rain index (*SMRI*) (red) for the accumulation period of 3 months.

elevational, seasonal, and inter annual variations. As *Shukla and Wood* [2008] stated, a runoff index complements the *SPI* and can serve to understand the actual hydrological situation concerning droughts. The *SRI* includes all runoff generation processes including snow melt in the modeled runoff. The strength of a runoff-based index is that it can be used for forecasting and is sensitive to hydrologic initial conditions such as snow conditions in spring [*Shukla and Wood*, 2008]. However, simulated grid runoff cannot be validated. Validation of the *SMRI* approach with *SSI* from streamflow observations in mesoscale catchments across a gradient of increasing snow influence, as proposed in

this study, shows that for these cases the simpler approach is a suitable alternative to describe the evolution of hydrological drought situations.

5. Conclusions

The *SMRI*, as introduced in this study, combines the low data requirements of the *SPI* with the explicit consideration of snow accumulation and melt. The analyses of the new index demonstrates its usefulness to indicate hydrological droughts in snow-influenced catchments, with specific advantages in those climatic
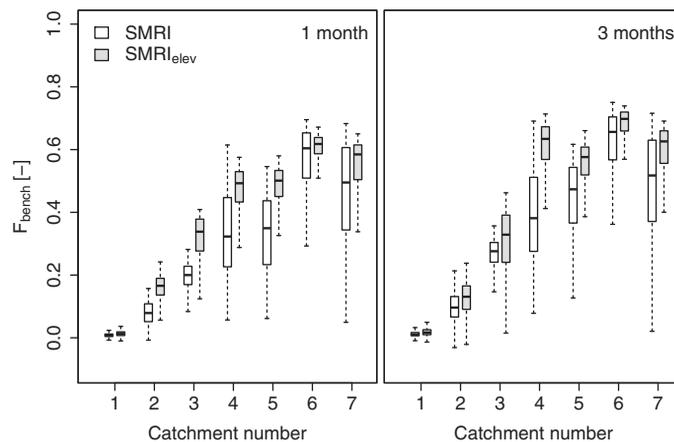
Figure 8. Comparison of the distribution of the measure of comparison for *SMRI* and *SMRI*$_{elev}$ for the aggregation periods of 1 (left) and 3 (right) months. Boxplots as in Figure 1.

regions where snow melt and rainy season coincide. This case study with Swiss catchments suggests a closer description of hydrological droughts by the *SMRI* than by *SPI*. Following the gradient of snow influence, the more a catchment is influenced by snow the more worthwhile it is to complement the *SPI* with the *SMRI*.

The *SMRI* is a somewhat more complex index than the *SPI* as it also uses temperature data to consider snow processes in the

computation. Thus it has some additional sources of uncertainty. The aggregation period can be adjusted to the typical seasonality of the hydrological regime, water resources use, and management requirements. As the index corresponds to the *SPI* during seasons or years without snow, it can be used without problems for drought monitoring and assessment over diverse mountain regions with regime transitions.

Despite the different realizations derived from different parameter sets of the snow model, the *SMRI* described both the hydrological situation in general as well as dry periods in particular closer than the *SPI* particularly in snow-influenced catchments. We therefore recommend using the *SMRI* for drought monitoring in snow-influenced catchments without streamflow measurements.

Appendix A: Snow Model

The new *SMRI* was based on snow melt computations using a simple degree-day snow model. Whenever the observed air temperature (T) ($^\circ$C) is lower than a threshold temperature (T_T) ($^\circ$C) precipitation is added to the snow storage (accumulation A [mm]). In addition to the accumulation, the liquid water content S_{liquid} (mm) in the snow pack is also calculated. S_{liquid} is calculated accounting for precipitation (P) (mm), melt M (mm), and refreezing (R) (mm) and has an upper bound constrained by the water holding capacity (C_{WH})(-). Refreezing (R) is determined by S_{liquid} of the day before, a degree-day factor C_M (mm/day$^\circ$C) and a refreezing factor C_{FR} (-). Melt is constrained by the preceding accumulation and calculated using C_M, T_T, and T. The contribution to surface runoff Q (mm) is all water that exceeds C_{WH} of the snow pack. For this study, C_{WH} was kept constant at a value of 0.1. (see pseudocode below)

if $T(t) < T_T$ **then**

   $R(t) = min(S_{liquid}(t-1), C_{FR} * C_M * (T_T - T(t)))$

   $A(t) = A(t-1) + P(t) + R(t)$

   $S_{liquid}(t) = S_{liquid}(t-1) - R(t)$

else

   $M(t) = min(A(t-1), C_M * (T(t) - T_T))$

   $A(t) = A(t-1) - M(t)$

   $S_{liquid}(t) = S_{liquid}(t-1) + P(t) + M(t)$

   if $S_{liquid}(t) > C_{WH} * A(t)$ **then**

      $Q(t) = S_{liquid}(t) - C_{WH} * A(t)$

      $S_{liquid}(t) = C_{WH} * A(t)$

   end if

end if

References

Bergström, S., J. Harlin, and G. Lindström (1992), Spillway design floods in Sweden: I. New guidelines, *Hydrol. Sci. J.*, *37*(5), 505–519.

Cancelliere, A., and J. D. Salas (2010), Drought probabilities and return period for annual streamflows series, *J. Hydrol.*, *391*(1), 77–89.

Choi, H. T., and K. Beven (2007), Multi-period and multi-criteria model conditioning to reduce prediction uncertainty in an application of topmodel within the glue framework, *J. Hydrol.*, *332*(3), 316–336.

Demaria, E. M., B. Nijssen, and T. Wagener (2007), Monte Carlo sensitivity analysis of land surface parameters using the variable infiltration capacity model, *J. Geophys. Res.*, *112*, D11113, doi:10.1029/2006JD007534.

Doesken, N. J., T. B. McKee, and J. D. Kleist (1991), Development of a surface water supply index for the western United States, final report 91–3, Dep. of Atmos. Sci., Colo. State Univ., Fort Collins, Colo.

Esko, K. (1980), On the values and variability of degree-day melting factor in Finland, *Nord. Hydrol.*, *11*(5), 235–242.

Federal Office for the Environment (2012), *Federal Office for the Environment*, Sect. of Hydrol. [Available at http://www.hydrodaten.admin.ch/en/index.html?lang=en, last accessed: 12.12.2012.]

Frei, C. (2013), Interpolation of temperature in a mountainous region using nonlinear profiles and non-Euclidean distances, *Int. J. Climatol.*, *34*, 1585–1605.

Ghosh, S., and P. Mujumdar (2007), Nonparametric methods for modeling GCM and scenario uncertainty in drought assessment, *Water Resour. Res.*, *43*(7), W07405, doi:10.1029/2006WR005351.

Guttman, N. (1999), Accepting the standardized precipitation index: a calculation algorithm, *J. Am. Water Resour. Assoc.*, *35*(2), 311–322.

Haslinger, K., D. Koffler, W. Schöner, and G. Laaha (2014), Exploring the link between meteorological drought and streamflow: Effects of climate-catchment interaction, *Water Resour. Res.*, *50*, 2468–2487, doi:10.1002/2013WR015051.

Hayes, M. J., M. D. Svoboda, D. A. Wilhite, and O. V. Vanyarkho (1999), Monitoring the 1996 drought using the standardized precipitation index, *Bull. Am. Meteorol. Soc.*, *80*(3), 429–438.

Heim, R., Jr. (2002), A review of twentieth-century drought indices used in the united states, *Bull. Am. Meteorol. Soc.*, *83*(8), 1149–1165.

Hock, R. (2003), Temperature index melt modelling in mountain areas, *J. Hydrol.*, *282*(1), 104–115.

Hosking, J. (1990), L-moments: analysis and estimation of distributions using linear combinations of order statistics, *J. R. Stat. Soc. Ser. B.*, *52*(1), 105–124.

Ji, L., and A. Peters (2003), Assessing vegetation response to drought in the northern great plains using vegetation and drought indices, *Remote Sens. Environ.*, *87*(1), 85–98.

Lindström, G. (1997), A simple automatic calibration routine for the HBV model, *Nord. Hydrol.*, *28*(3), 153–168.

Lindström, G., B. Johansson, M. Persson, M. Gardelin, and S. Bergström (1997), Development and test of the distributed hbv-96 hydrological model, *J. Hydrol.*, *201*(1), 272–288.

López-Moreno, J., S. Vicente-Serrano, S. Beguería, J. García-Ruiz, M. Portela, and A. Almeida (2009), Downstream propagation of hydrological droughts in highly regulated transboundary rivers: The case of the Tagus river between Spain and Portugal, *Water Resour. Res.*, *45*, W02405, doi:10.1029/2008WR007198.

McKee, T., N. Doesken, and J. Kleist (1993), The relationship of drought frequency and duration to time scales, in *Proceedings of the 8th Conference on Applied Climatology*, vol. 17, pp. 179–183, Am. Meteorol. Soc., Boston, Mass.

Merz, R., and G. Blöschl (2004), Regionalisation of catchment model parameters, *J. Hydrol.*, *287*(1), 95–123.

Montanari, A. (2005), Large sample behaviors of the generalized likelihood uncertainty estimation (glue) in assessing the uncertainty of rainfall-runoff simulations, *Water Resour. Res.*, *41*, W08406, doi:10.1029/2004WR003826.

Naresh Kumar, M., C. Murthy, M. Sesha Sai, and P. Roy (2009), On the use of standardized precipitation index (spi) for drought intensity assessment, *Meteorol. Appl.*, *16*(3), 381–389.

Orlowsky, B., and S. I. Seneviratne (2012), Global changes in extreme events: Regional and seasonal dimension, *Clim. Change*, *110*(3), 669–696.

Pappenberger, F., and K. J. Beven (2004), Functional classification and evaluation of hydrographs based on multicomponent mapping (Mx), *Int. J. River Basin Manage.*, *2*(2), 89–100.

Rasmussen, R., et al. (2012), How well are we measuring snow: The NOAA/FAA/NCAR winter precipitation test bed, *Bull. Am. Meteorol. Soc.*, *93*(6), 811–829.

Rebetez, M., H. Mayer, O. Dupont, D. Schindler, K. Gartner, J. P. Kropp, and A. Menzel (2006), Heat and drought 2003 in Europe: A climate synthesis, *Ann. Forest Sci.*, *63*(6), 569–577.

Schaefli, B., and H. V. Gupta (2007), Do Nash values have value?, *Hydrol. Processes*, *21*(15), 2075–2080.

Seibert, J. (1999), Regionalisation of parameters for a conceptual rainfall-runoff model, *Agric. Forest Meteorol.*, *98*, 279–293.

Seibert, J. (2000), Multi-criteria calibration of a conceptual runoff model using a genetic algorithm, *Hydrol. Earth Syst. Sci.*, *4*(2), 215–224.

Seibert, J., and M. Vis (2012), Teaching hydrological modeling with a user-friendly catchment-runoff-model software package, *Hydrol. Earth Syst. Sci.*, *16*(9), 3315–3325.

Shafer, B., and L. Dezman (1982), Development of a surface water supply index (SWSI) to assess the severity of drought conditions in snowpack runoff areas, in Proceedings of the Western Snow Conference, vol. 50, pp. 164–175, Western Snow Conference, Reno, Nev.

Shukla, S., and A. Wood (2008), Use of a standardized runoff index for characterizing hydrologic drought, *Geophys. Res. Lett.*, *35*(2), L02405, doi:10.1029/2007GL032487.

Uhlenbrook, S., J. Seibert, C. Leibundgut, and A. Rodhe (1999), Prediction uncertainty of conceptual rainfall-runoff models caused by problems in identifying model parameters and structure, *Hydrol. Sci. J.*, *44*(5), 779–797.

Van Loon, A., and H. Van Lanen (2012), A process-based typology of hydrological drought, *Hydrol. Earth Syst. Sci.*, *16*(7), 1915–1946.

van Vliet, M. T., J. R. Yearsley, F. Ludwig, S. Vögele, D. P. Lettenmaier, and P. Kabat (2012), Vulnerability of us and European electricity supply to climate change, *Nat. Clim. Change*, *2*(9), 676–681.

Vicente-Serrano, S., S. Beguería, and J. López-Moreno (2010), A multiscalar drought index sensitive to global warming: The standardized precipitation evapotranspiration index, *J. Clim.*, *23*(7), 1696–1718.

Vicente-Serrano, S., J. López-Moreno, S. Beguería, J. Lorenzo-Lacruz, C. Azorin-Molina, and E. Morán-Tejeda (2011), Accurate computation of a streamflow drought index, *J. Hydrol. Eng.*, *17*(2), 318–332.

Vicente-Serrano, S. M., S. Beguería, J. Lorenzo-Lacruz, J. J. Camarero, J. I. López-Moreno, C. Azorin-Molina, J. Revuelto, E. Morán-Tejeda, and A. Sanchez-Lorenzo (2012), Performance of drought indices for ecological, agricultural, and hydrological applications, *Earth Interact.*, *16*, 1–27, doi:10.1175/2012EI000434.1.

Vidal, J., E. Martin, L. Franchistéguy, F. Habets, J. Soubeyroux, M. Blanchard, M. Baillon (2010), Multilevel and multiscale drought reanalysis over France with the Safran-Isba-Modcou hydrometeorological suite, *Hydrol. Earth Syst. Sci.*, *14*(3), 459–478.